

Modeling Contact Resistivity in Monolayer Molybdenum disulfide Edge contacts

Madhuchhanda Brahma*, Maarten L. Van de Put*, Edward Chen[†],
Massimo V. Fischetti*, and William G. Vandenberghe*

**Department of Materials Science and Engineering, The University of Texas at Dallas,
800 W. Campbell Rd., Richardson, Texas 75080, USA.*

*[†]Corporate Research, Taiwan Semiconductor Manufacturing Company Ltd.,
168, Park Ave. II, Hsinchu Science Park, Hsinchu 300-75, Taiwan.*

Email: madhuchhanda.brahma@utdallas.edu, maarten.vandepu@utdallas.edu, chenjhm@tsmc.com,
max.fischetti@utdallas.edu, william.vandenberghe@utdallas.edu

Abstract—We calculate the resistivity of Schottky edge contacts between a metal and a transition-metal dichalcogenide (TMD) thin layer. The electrostatic potential is obtained by solving numerically the Poisson equation; the transmission probability is computed using the Wentzel–Kramers–Brillouin (WKB) approximation using the full-band density of states obtained from density functional theory (DFT); the effect of the image force is obtained analytically using the Green’s function for the Poisson equation with boundary conditions appropriate to the geometry we have considered. We find that the dielectric environment surrounding the 2D layer largely controls the electrostatics and image-force barrier lowering. Low-resistance metal-TMD Schottky edge contacts are obtained using low- κ top and bottom insulators.

Index Terms—metal/TMD, edge contact, WKB, 2D Poisson, image force, dielectric

I. INTRODUCTION

A low contact-resistance is desirable for obtaining a high on-current in field-effect transistors (FETs) based on TMD layers. However, metal/TMD contacts are characterized by high Schottky barriers [1]–[5] which severely limit the drive current in such devices. Semiconducting MoS₂, one of the widely studied TMD channel materials in 2D FETs, is usually affected by a contact resistivity larger than 1 k Ω μ m [1]–[4]. One of the lowest contact resistances reported for multi-layer MoS₂ FETs is 0.54 k Ω μ m with an on-current of 830 μ A/ μ m at 300 K [6]. Though there has been an extensive experimental investigation of the contact geometry in 2D FETs, theoretical studies are limited. Therefore, a physical understanding of the carrier-injection mechanism for practical device configurations still needs to be developed. A model incorporating ab initio quantum transport simulations to predict the influence of transfer length, interfacial oxide on the carrier injection process through metal-TMD contacts has been reported recently

[7]. Other studies on the modeling of the resistance of metal-TMD contacts employ a simplified picture [8], [9]. None of the studies account for effect of the surrounding dielectrics, an effect which is known to be important in such 2D geometry [10], [11].

Here we present results obtained using a theoretical and numerical model to evaluate contact resistance in realistic metal-2D edge contact in which the resistivity is controlled mainly by the Schottky barrier. Our model uses the full-band density of states obtained from DFT calculations for MoS₂ and the WKB approximation to calculate the transmission probability through the Schottky barrier at the metal-MoS₂ interface. We organize the presentation as follows: We first describe the numerical and mathematical approach to solve the contact resistance starting from DFT calculations. Next, we present our results, discussing the values of the contact resistance we have obtained, emphasizing the role played by the different choices of parameters we have used. Finally, we draw our conclusions.

II. METHOD

DFT calculations have been performed using the Vienna Ab initio Simulation Package (VASP) [12]–[15]. We have employed the generalized gradient approximation (GGA) with the projector augmented wave (PAW) method [16] using the Perdew-Burke-Ernzerhof (PBE) exchange-correlation functional [17] and the Heyd-Scuseria-Ernzerhof (HSE06) hybrid functional [18]. DFT-D3 dispersion correction of Grimme [19] was used to describe van der Waals interactions and accurately calculate the interlayer distance. A cut-off energy of 400 eV has been used. We sampled the Brillouin zone with Γ -centered 25 \times 25 \times 1 and 10 \times 10 \times 6 k-meshes in monolayer and bulk MoS₂ respectively. We set the electronic convergence at 10⁻⁶eV whereas the structural geometry was optimized until the maximum force on every atom fell below 0.01 eV/Å. A large vacuum

padding of 30Å was used along the z direction to avoid interaction between adjacent layers.

In Fig. 1 we illustrate the geometry we have considered: A semi-infinite TMD monolayer material is sandwiched between very thick top and bottom dielectrics ($t_{\text{dielectric}} \gg t_{2\text{D}}$), with a metal contact at the left. We assume the contact to clamp the potential at the metal-TMD/metal-oxide interface; that is, the metal is assumed to be region of constant potential. We have

$$\frac{1}{\rho_c} = \int_{-\infty}^{\infty} \frac{2e^2}{h} \left\{ \int \left[\sum_n \left(\int \delta[E - E_n(k_y)] dE_n(k_x, k_y) \right) T_n(k_y, E) \right] \frac{dk_y}{(2\pi)} \right\} \frac{-\partial f(E)}{\partial E} dE \quad (1)$$

where ρ_c is the resistivity, e is electronic charge, h is Planck's constant, $f(E)$ is the fermi distribution at energy E and (k_x, k_y) are wave vectors. The Bloch

considered the specific case of n-type monolayer MoS₂ as channel material, but the results will apply to other TMDs as well. We consider transport along the x direction and translational invariance along the y direction. Anisotropic dielectric permittivity values are considered for monolayer MoS₂ [20].

The Schottky-barrier-limited contact resistivity [21] has been calculated from the ballistic conductance of the monolayer TMD, modulated by the Schottky barrier according to the following equation:

$$T_n(k_y, E) = \exp \left(-2 \int_0^{x_{\text{max}}} \sqrt{\frac{2m_n^*(k_y)}{\hbar^2} [E - U(x) - E_{n,\text{min}}(k_y)]} dx \right) \quad (2)$$

where, $m_n^*(k_y)$ and $E_{n,\text{min}}(k_y)$ are the effective mass and the energy band dispersion minimum, respectively, as a function of k_y for the n th conducting mode, x_{max} is the maximum length of the depletion potential, E is the energy of the carriers, $U(x)$ is the Schottky depletion potential with built-in potential barrier $\phi_{\text{bi}} = (\phi_{\text{M}} - \chi_{\text{S}}) - (E_{\text{C}} - E_{\text{F}})$, where ϕ_{M} , χ_{S} , E_{C} and E_{F} are the metal work function, monolayer TMD electron affinity, conduction band edge and Fermi level respectively.

The potential was computed by solving 2D Poisson's equation (in the (x, z) plane) self consistently with the full-band density of states using a finite-elements based package FEniCS [22], [23]. Dirichlet boundary

wave dispersion, $E_n(k_x, k_y)$, is obtained from the DFT calculations in VASP, and n stands for each conducting mode. The transmission probability was calculated using the WKB approximation as follows:

conditions were imposed at the metal contact side and Neumann boundary conditions on the other sides (thus ignoring any effect of a gate bias). The 2D Poisson's equation is as follows:

$$\nabla \cdot \nabla[\epsilon_o \epsilon(r) V(r)] = e(N_{\text{D}} - \rho) \quad (3)$$

where, N_{D} and ρ are doping concentration and electron density respectively, $V(r)$ is the potential energy and $\epsilon(r)$ the spatially varying dielectric permittivity in the geometry shown in Fig. 1.

For calculating image force barrier lowering, we first compute the Coulomb kernel for a charge particle in the middle for the configuration shown in Fig. 2.

$$\hat{V}(Q, z=0) = -\frac{2e^{2a\beta Q} [\epsilon_{2\text{D}} \cosh(a\beta Q) + \epsilon_{\text{bot}} \sinh(a\beta Q)] [\epsilon_{2\text{D}} \cosh(a\beta Q) + \epsilon_{\text{top}} \sinh(a\beta Q)]}{\epsilon_{2\text{D}} Q [(\epsilon_{2\text{D}} - \epsilon_{\text{top}})(\epsilon_{\text{bot}} - \epsilon_{2\text{D}}) + (\epsilon_{2\text{D}} + \epsilon_{\text{top}})(\epsilon_{2\text{D}} + \epsilon_{\text{bot}}) e^{4a\beta Q}]} \quad (4)$$

where, ϵ_{top} and ϵ_{bot} are the top ($z > a$) and bottom ($z < a$) oxide dielectric permittivity, the thickness of the middle 2D layer ($-a < z < a$) is $2a$, $\epsilon_{2\text{D}} = \sqrt{\epsilon_{\parallel} \epsilon_{\perp}}$ and $\beta = \sqrt{\frac{\epsilon_{\parallel}}{\epsilon_{\perp}}}$, where ϵ_{\parallel} and ϵ_{\perp} are the in-plane and out-of-plane dielectric constants of monolayer MoS₂.

Finally, the real space potential $V(x)$ at $(x, z=0)$ due to the point charge at $(x, z=0)$ is obtained numerically [24] by 2D Fourier-Bessel or Hankel transform of Eq.

(4) and is given as follows.

$$V(x) = \frac{e}{2\pi} \int_0^{\infty} \hat{V}(Q, z=0) J_0(xQ) Q dQ \quad (5)$$

where, J_0 is the Bessel function of the first kind of order zero.

For edge contacts, the method of images is used to account for the constant potential at the metal contact.

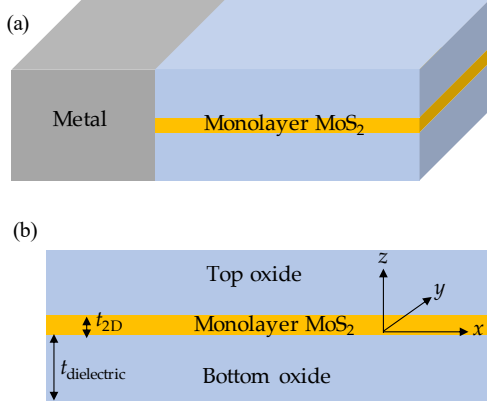


Fig. 1: (a) Edge contact geometry considered in our model. (b) 2D cross-section of the edge contact geometry (metal not shown). The middle layer is monolayer MoS₂ with a thickness t_{2D} , sandwiched between infinitely thick top and bottom insulators.

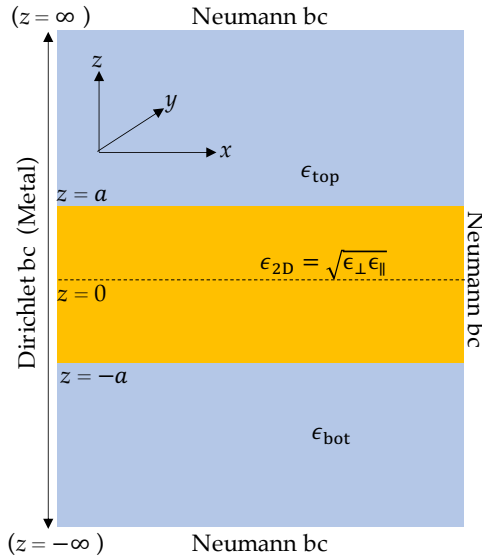


Fig. 2: Schematic of the system where we compute the Coulomb kernel with a point charge located at $z = 0$. The top and bottom oxides have a homogenous isotropic permittivity, whereas the middle (2D) semiconductor has anisotropic permittivity.

The image potential is the (negative) work done to bring a charge from infinity to a distance x from the metal-2D interface (at a distance $2x$ from the image charge) and is found to be equivalent to $1/2 V(2x)$. The image potential is then added to the depletion potential calculated numerically in order to obtain the total potential.

III. RESULTS AND DISCUSSION

Fig. 3 shows our main result, the calculated contact resistivity as a function of doping concentration in an edge contact MoS₂ monolayer with either SiO₂ or HfO₂ as top and bottom insulators, and bulk MoS₂, for a fixed Schottky-barrier height of 0.3 eV. We see increasing the

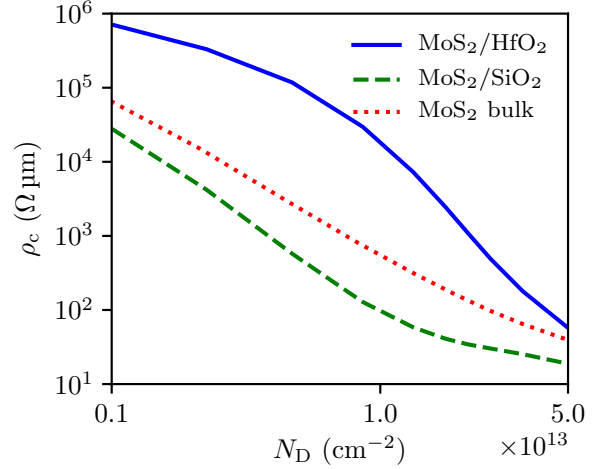


Fig. 3: Calculated contact resistivities for bulk and monolayer MoS₂ edge contacts. MoS₂ sandwiched between SiO₂ or HfO₂ labeled as MoS₂/SiO₂ and MoS₂/HfO₂ respectively.

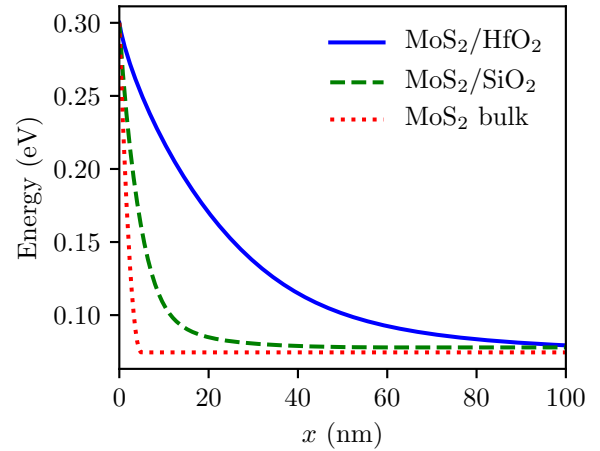


Fig. 4: Potential energy for MoS₂/SiO₂, MoS₂/HfO₂ and bulk, along the transport direction x for a Schottky barrier height of 0.3 eV and a doping concentration $N_D = 1 \times 10^{12}/\text{cm}^2$.

doping reduces the resistivity, a trend which is consistent with what is observed in metal/bulk-semiconductor contacts. Interestingly, we find that the presence of a low- κ surrounding dielectric, such as SiO₂, results in a lower resistivity than its bulk counterpart.

Indeed, the surrounding dielectrics affect very strongly the electrostatic behavior of such 2D geometries, controlling both the width of the depletion region as well as the barrier lowering due to the image force. The first effect is illustrated in Fig. 4 which shows the potential energy in the center of the MoS₂ channel. The depletion width is smallest in the bulk-TMD geometry and increases with increasing dielectric constant of the surrounding dielectrics, being largest in the case of HfO₂. Obviously,

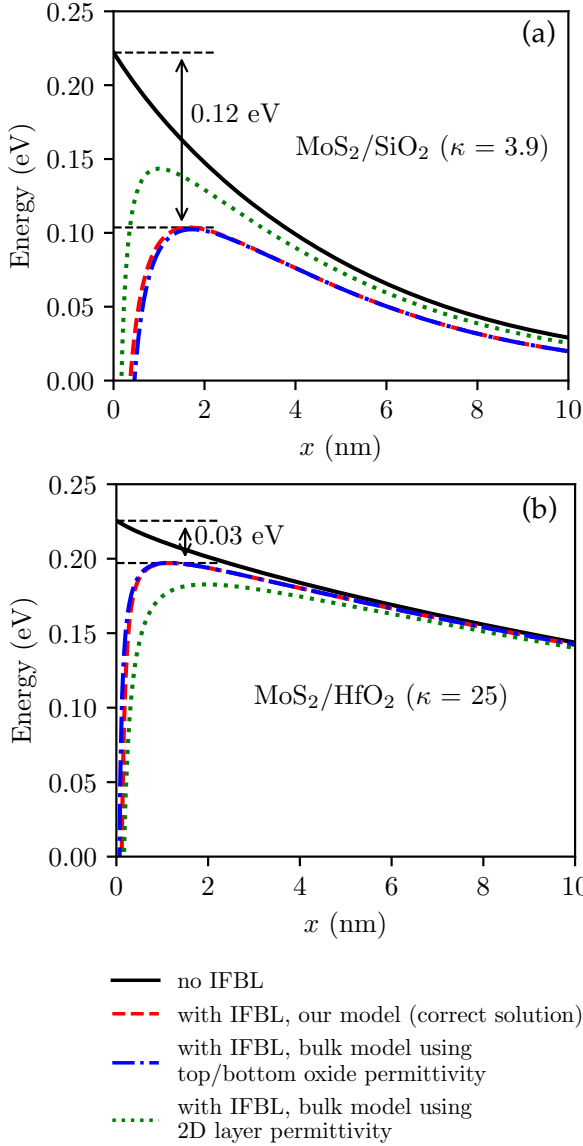


Fig. 5: Potential energy in the monolayer calculated ignoring image-force barrier-lowering (black solid line), the “correct” 2D solution (red dashed line), and the bulk model for the barrier lowering (blue dashed-dot and green dotted lines, using TMD or insulator permittivity, respectively), for a Schottky barrier height of 0.3 eV and a doping concentration $N_D = 1 \times 10^{12}/\text{cm}^2$, where top and bottom oxides are (a) SiO₂ and (b) HfO₂.

a larger depletion width results in a thicker tunneling barrier and, so, in a reduced transmission probability. This is reflected in higher values of contact resistance in MoS₂/HfO₂.

The second effect, the image force barrier lowering (IFBL), consists in the reduction in effective barrier height due to the image charges inside the metal contact, as required to maintain the metal region at a constant potential. The role played by the IFBL is illustrated in Fig. 5 that shows the potential energy as in Fig. 4, but

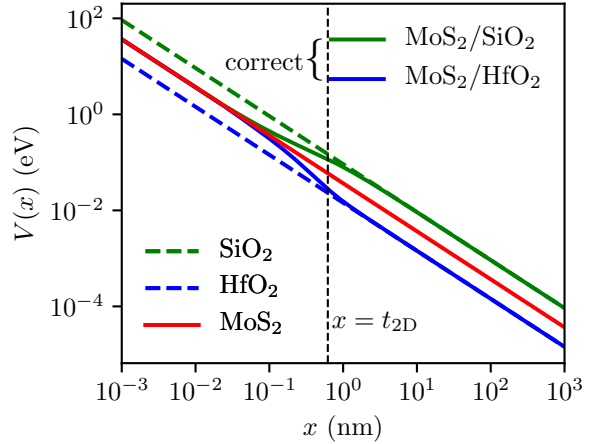


Fig. 6: The image potential plotted as a function of the distance from the metal-TMD interface in MoS₂/SiO₂ (correct solution), MoS₂/HfO₂ (correct solution), and using the conventional model with insulator permittivity (labeled as SiO₂ and HfO₂) or TMD permittivity (labeled as MoS₂). For $x \gg t_{2D}$, the conventional bulk model (using insulator permittivity) matches the correct solution but fails when $x \ll t_{2D}$.

now accounting for the IFBL for a fixed doping concentration in the two extreme cases of SiO₂ (Fig. 5(a)) and HfO₂ (Fig. 5(b)). The magnitude of barrier lowering is the difference between the peak of the no-IFBL and IFBL potential energies (shown by the arrow in Fig. 5). We find that barrier lowering is greater in MoS₂/SiO₂ than MoS₂/HfO₂ and leads to a reduction in contact resistivity. This results from the effect of surrounding dielectric on the image potentials.

Finally, we show in Fig. 6 image potential for a point charge located in the middle of the MoS₂ monolayer in the presence of different surrounding dielectrics. The distance of the point charge from the metal interface is denoted by x , and $V(x)$ is the image potential. Asymptotically, we see that at distances much larger than the layer thickness ($x \gg t_{2D}$) the barrier potential behaves as $1/(\epsilon_{\text{dielectric}}x)$, whereas when $x \ll t_{2D}$, the 2D-material dielectric constant dominates, as in the bulk case, and the barrier-lowered potential behaves as $1/(\epsilon_{2D}x)$. When $x \approx t_{2D}$, a numerical evaluation is required to obtain the correct result.

IV. CONCLUSION

We have developed a numerical model to study the carrier injection mechanism through the Schottky barrier at metal/2D-layer edge contacts and calculate the contact resistance. We have shown how the surrounding dielectric environment largely controls the electrostatics in this 2D geometry by considering cases with both low- and high- κ top and bottom oxides. We have shown that low- κ top and bottom insulators help in reducing the resistance, thanks to a smaller depletion width and a higher image-

force barrier-lowering. Indeed, we have found that the image-force barrier-lowering in these edge contacts is determined by the dielectric permittivity of both the surrounding oxide(s) and of the TMD. This contrasts with bulk devices in which only the permittivity of the semiconductor determines the magnitude of the barrier lowering

ACKNOWLEDGMENT

This work has been supported by the Taiwan Semiconductor Manufacturing Company, Ltd. and the NEWLIM-ITS/nCORE program of the Semiconductor Research Corporation (SRC).

REFERENCES

- [1] S. Das, and J. Appenzeller, "Where does the current flow in two-dimensional layered systems?," *Nano letters*, vol. 13, pp. 3396–402, Jul 2013.
- [2] H. Liu, M. Si, Y. Deng, A. T. Neal, Y. Du, S. Najmaei, P. M. Ajayan, J. Lou, and P. D. Ye, "Switching mechanism in single-layer molybdenum disulfide transistors: An insight into current flow across Schottky barriers," *ACS nano.*, vol. 8, pp. 1031–1038, Jan 2014
- [3] Y. Guo Y, Y. Han, J. Li, A. Xiang, X. Wei, S. Gao, and Q. Chen, "Study on the resistance distribution at the contact between molybdenum disulfide and metals," *ACS nano.*, vol. 8, pp. 7771–7779, Aug 2014.
- [4] A. Allain, J. Kang, K. Banerjee, and A. Kis, "Electrical contacts to two-dimensional semiconductors," *Nature materials*, vol. 14, pp. 1195–1205, Dec. 2015.
- [5] D. S. Schulman, A. J. Arnold, and S. Das, "Contact engineering for 2D materials and devices," *Chemical Society Reviews*, vol. 47, pp. 3037–3058, Mar 2018.
- [6] Y. Liu, J. Guo, Y. Wu, E. Zhu, N. O. Weiss, Q. He, H. Wu, H. C. Cheng, Y. Xu, I. Shakir, and Y. Huang, "Pushing the performance limit of sub-100 nm molybdenum disulfide transistors," *Nano letters*, vol. 16, pp. 6337–6342, Oct 2016.
- [7] A. Szabo, A. Jain, M. Parzefall, L. Novotny, and M. Luisier, "Electron transport through metal/MoS₂ interfaces: edge-or area-dependent process?," *Nano letters*, vol. 19, pp. 3641–3647, May 2019.
- [8] V. Mishra and S. Salahuddin, "Intrinsic limits to contact resistivity in transition metal dichalcogenides," *IEEE Electron Device Letters*, vol. 38, pp. 1755–1758, Oct 2017.
- [9] D. Wickramaratne, F. Zahid, and R. K. Lake, "Electronic and thermoelectric properties of few-layer transition metal dichalcogenides," *The Journal of chemical physics*, vol. 140, p. 124710, Mar 2014.
- [10] A. Nipane, S. Jayanti, A. Borah, and J. T. Teherani, "Electrostatics of lateral pn junctions in atomically thin materials," *Journal of Applied Physics*, vol. 122, p.194501, Nov 2017.
- [11] H. Ilatikhameneh, T. Ameen, F. Chen, H. Sahasrabudhe, G. Klimeck, and R. Rahman, "Dramatic impact of dimensionality on the electrostatics of pn junctions and its sensing and switching applications," *IEEE Transactions on Nanotechnology*, vol. 17, pp. 293–298, Jan 2018.
- [12] G. Kresse and J. Hafner, "Ab initio molecular dynamics for liquid metals," *Physical review B*, vol., p. 558, Jan 1993.
- [13] G. Kresse, and J. Hafner, "Ab initio molecular-dynamics simulation of the liquid-metal-amorphous-semiconductor transition in germanium," *Physical Review B*, vol. 49, p.14251, May 1994.
- [14] G. Kresse, and J. Furthmuller, "Efficient iterative schemes for ab initio total-energy calculations using a plane-wave basis set," *Physical review B*, vol. 54, p. 11169, 1996.
- [15] G. Kresse, and J. Furthmuller, "Efficiency of ab-initio total energy calculations for metals and semiconductors using a plane-wave basis set.," *Computational materials science*, vol. 6, pp.15–50, 1996.
- [16] G. Kresse, and D. Joubert, "From ultrasoft pseudopotentials to the projector augmented-wave method," *Physical Review B*, vol. 59, p. 1758, 1999.
- [17] J. P. Perdew, K. Burke, and M. Ernzerhof, "Generalized gradient approximation made simple," *Physical review letters*, vol. 77, p. 3865, 1996
- [18] J. Heyd, G. E. Scuseria, and M. Ernzerhof, "Hybrid functionals based on a screened coulomb potential," *The Journal of chemical physics*, vol. 118, pp. 8207–8215, 2003.
- [19] S. Grimme, J. Antony, S. Ehrlich, and H. Krieg, "A consistent and accurate ab initio parametrization of density functional dispersion correction (dft-d) for the 94 elements h-pu," *The Journal of chemical physics*, vol. 132, p.154104, 2010.
- [20] A. Laturia, M. L. Van de Put, and W. G. Vandenberghe., "Dielectric properties of hexagonal boron nitride and transition metal dichalcogenides: from monolayer to bulk," *npj 2D Materials and Applications*, vol. 2, pp. 1–7, Mar 2018.
- [21] S. Ravandi, B. Fu, W. G. Vandenberghe, S. J. Aboud, and M. V. Fischetti, "Pseudopotential-based study of gate leakage and contact resistance beyond the 10 nm node," 16th International Workshop on Computational Electronics, Nara, Japan, Jun 2013.
- [22] M. S. Alnaes, J. Blechta, J. N. Hake, A. Johansson, B. Kehlet, A. Logg, C. Richardson, J. Ring, M. E. Rognes, and G. N. Wells., "The fenics project version 1.5." *Archive of Numerical Software*, 3(100), 2015.
- [23] A. Logg, K. A. Mardal, G. N. Wells, et al. "Automated Solution of Differential Equations by the Finite Element Method," Springer, 2012.
- [24] S. G. Murray and F. J. Poulin, "hankel: A python library for performing simple and accurate hankel transformations," arXiv preprint arXiv:1906.01088, 2019.